



## Removal of roxarsone from aqueous solution by Fe/La-modified montmorillonite

Ya-Jiao Wang<sup>a</sup>, Feng Ji<sup>b</sup>, Wei Wang<sup>a,c</sup>, Shou-Jun Yuan<sup>a,c</sup>, Zhen-Hu Hu<sup>a,c,\*</sup>

<sup>a</sup>School of Civil Engineering, Hefei University of Technology, Hefei 230009, China, Tel. +86 551 62904144; email: wyajiao55@163.com (Y.-J. Wang), Tel. +86 551 62904148; emails: dwhit@163.com (W. Wang),

sjyuan@hfut.edu.cn (S.-J. Yuan), Tel. +86 551 62904144; Fax: +86 551 62902066; email: zhhu@hfut.edu.cn (Z.-H. Hu)

<sup>b</sup>Institute of Animal Husbandry and Veterinary Medicine, Beijing Academy of Agriculture and Forestry Sciences, Beijing 100097, China, Tel. +86 010 51503301; email: fengjp3@hotmail.com

<sup>c</sup>Institute of Water Treatment and Wastes Reutilization, School of Civil Engineering, Hefei University of Technology, Hefei 230009, China

Received 26 April 2015; Accepted 11 October 2015

### ABSTRACT

Roxarsone is an organoarsenical compound widely used as a feed additive in animal husbandry and might result in the contamination of inorganic arsenic in aquatic environment. Montmorillonite is an economical adsorbent with many advantages. In this study, Fe/La-modified montmorillonite (Fe/La-Mt) was prepared, characterized, and investigated for the removal of roxarsone from aqueous solutions. Brunauer–Emmett–Teller (BET) analysis confirmed the increase in specific surface area and pore volume of montmorillonite after modification. FESEM analysis showed that Fe/La-Mt formed flake structure and the structure was collapsed after being calcined (C-Fe/La-Mt). The adsorption results indicated that the adsorption capacity of Fe/La-Mt onto roxarsone is higher than that of C-Fe/La-Mt. The adsorption process of roxarsone onto Fe/La-Mt and C-Fe/La-Mt can be well described using pseudo-second-order model and interpreted using the Langmuir isotherm. Thermodynamic analysis indicated that the adsorption was a spontaneous and endothermic process. The adsorption capacity reduced slightly when solution pH increased from 2.5 to 8.0. The ion of  $\text{PO}_4^{3-}$  greatly decreased the adsorption of roxarsone onto Fe/La-Mt. X-ray photoelectron spectroscopy analysis confirmed the loading of arsenic (V) onto the surface of Fe/La-Mt. The high adsorption capacity in a wide pH range demonstrated that Fe/La-Mt can be used potentially for the removal of roxarsone from aqueous solution.

*Keywords:* Adsorption; Fe/La-modified montmorillonite; Removal; Roxarsone

### 1. Introduction

Roxarsone (4-hydroxy-3-nitrophenylarsonic acid, Fig. 1) has been widely used in broiler husbandry to treat coccidiosis and to improve feed efficiency since

the US Food and Drug Administration (FDA) approved its use as an additive in 1944 [1]. The permitted dose in broiler feed was  $50 \text{ mg kg}^{-1}$  [1]. The usage of roxarsone was approximately 1,000 tons annually in the United States, and more in China [1,2]. Most of the added roxarsone is excreted with feces without chemical change. It is slowly converted into

\*Corresponding author.

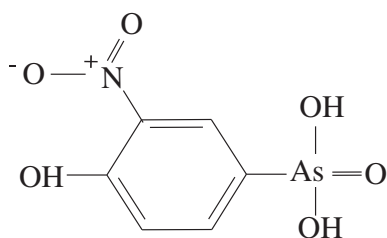


Fig. 1. Chemical structural formula of roxarsone.

more mobile and toxic inorganic arsenics through biological and/or chemical process once released into the environment through wastewater or land application [3–5], causing arsenic contamination [6]. The chronic exposure to arsenic may cause cancer. Arsenic contamination has become one of the major environmental concerns [7], and the WHO has lowered the maximum concentration of arsenic in drinking water from 50 to 10  $\mu\text{g L}^{-1}$  [8]. Therefore, the removal of roxarsone from wastewater is very important to avoid the contamination of inorganic arsenics.

The removal of inorganic arsenic from aqueous solution has been widely investigated [9,10]. Researchers have also paid attention to the removal of organic arsenics from animal husbandry in recent years and many methods have been investigated such as adsorption [11], photo-degradation [12,13], and biotransformation [2,14–16]. Among these methods, adsorption removal was considered as an economical way due to its low cost, high efficiency, and easy handling [17]. Suitable adsorbent is the key issue for the adsorption removal.

Montmorillonites are abundant in nature and widely used as adsorbents for its characteristics of high specific surface area, chemical and physical stabilities, high cation-exchange capacity (CEC), and low

cost [18]. However, natural montmorillonite still has limitations on the adsorption of organic and inorganic compounds [18]. Many modification methods have been applied in recent years for improving the adsorption efficiency, such as the use of organic or inorganic modifiers, as summarized in Table 1 [18–24].

Recent studies have shown that modified montmorillonite can remove inorganic arsenic from aqueous solutions [22,25]. Iron(III) oxides/hydroxides such as goethite ( $\alpha\text{-FeOOH}$ ) and hydrous ferric oxide have been reported to be promising adsorbents for removing inorganic arsenic compounds [17], and lanthanum-loaded zeolite enhanced the removal of arsenate [26]. The addition of lanthanum in clays also enhanced the adsorption of fluorine and phosphate [27,28]. Roxarsone contains an arsenate moiety and aromatic ring which are bonded through an arsenic–carbon bond [6], thus La/Fe-based materials might also show high affinities toward roxarsone [29]. However, little is known about the removal of roxarsone through La/Fe-modified clays.

In this study, montmorillonite was modified by a hydrolysis method, and the pillaring agents were prepared using  $\text{Fe}(\text{NO}_3)_3 \cdot 9\text{H}_2\text{O}$  and  $\text{La}(\text{NO}_3)_3 \cdot n\text{H}_2\text{O}$ . The aim of this study was to: (1) characterize the original and modified montmorillonites, (2) investigate the adsorption removal of roxarsone through modified montmorillonites, and (3) analyze the adsorption kinetics and isotherms of roxarsone onto modified montmorillonites.

## 2. Materials and methods

### 2.1. Materials

Calcium-montmorillonites (Ca-Mt) used in this study was purchased from Wuhuatianbao mineral

Table 1  
Methods and modifiers of modification for montmorillonite in recent years

Raw montmorillonite		Modified montmorillonite		Modifiers	Adsorbates	Refs.
(0 0 1) spacing of XRD (nm)	$S_{\text{BET}}$ ( $\text{m}^2 \text{g}^{-1}$ )	(0 0 1) spacing of XRD (nm)	$S_{\text{BET}}$ ( $\text{m}^2 \text{g}^{-1}$ )			
0.96	183.2	1.17	175	Ionic liquid (1-methyl, 3-decahexyl imidazolium)	Amaranth dye	[18]
1.55		1.73		Dodecyl sulfobetaine	Methylene blue, $\text{Cu}^{2+}$	[19]
1.21		1.44		Cetyltrimethylammonium bromide	Acid orange 7	[20]
1.52		1.56–1.81		Hydroxy-iron	Arsenic	[21]
1.25	9.79	Exfoliated	16.08	Polypyrrole	$\text{Cr}^{6+}$	[22]
	71.15		154.17	Ethylamine	$\text{Cs}^+$	[23]
1.56		15.8		Humic acid	$\text{Cu}^{2+}$ , $\text{Cd}^{2+}$ , $\text{Cr}^{3+}$	[24]

materials Co., Ltd, Inner Mongolia with CEC of 53.0 mmol/100 g. The components of Ca-Mt were (wt.%): SiO<sub>2</sub>, 56.57; Al<sub>2</sub>O<sub>3</sub>, 17.36; Fe<sub>2</sub>O<sub>3</sub>, 4.34; CaO, 2.04; MgO, 4.31; K<sub>2</sub>O, 0.24; Na<sub>2</sub>O, 0.28; MnO, 0.066; and TiO<sub>2</sub>, 0.24. Roxarsone (purity > 99%) was purchased from Sigma-Aldrich, China. A stock solution of roxarsone (100.0 mg L<sup>-1</sup>) was prepared in deionized water and stored in a brown reagent bottle. Other chemicals used in this work were of analytical reagent grade.

## 2.2. Preparation of Na-montmorillonite and Fe/La-pillared montmorillonite

Na-montmorillonite (Na-Mt) was produced from Ca-Mt, as described by Yuan et al. [30]. Twenty grams of raw Ca-Mt and 0.8 g of Na<sub>2</sub>CO<sub>3</sub> were mixed with 400 mL of deionized water. The mixture was stirred vigorously at 80°C for 2 h, followed by eight cycles of centrifugation and washing. After discharging the supernatant, the Na-Mt was collected and dried at 105°C. Then, the dried solid was ground and passed through a 100-mesh sieve.

Fe/La-pillared montmorillonite (Fe/La-Mt) was prepared from Na-Mt. Fe/La-Mt was synthesized according to the process reported by Yuan et al. [30]. The pillaring agent was prepared by slowly adding the powder Na<sub>2</sub>CO<sub>3</sub> (10.6 g) to 600 mL of mixed solution of 0.33 mol L<sup>-1</sup> Fe(NO<sub>3</sub>)<sub>3</sub> and 1.65 × 10<sup>-3</sup> mol L<sup>-1</sup> La(NO<sub>3</sub>)<sub>3</sub> with vigorous stirring for 2 h followed by 24 h of aging at room temperature. Then, the obtained pillaring agent was added dropwise into 2% Na-Mt at a ratio of Fe:Na-Mt = 1.0 mmol g<sup>-1</sup> of the modified clay. After the addition of pillaring agent, the obtained suspension was stirred for additional 2 h then followed by 20 h of aging at 70°C. After 8 successive cycles of washing and centrifugation, the collected solid was dried at 105°C for 24 h, ground and sieved through 100 meshes. The mass ratio of Fe:La:Na-Mt in Fe/La-Mt is 5.6:0.07:100. Finally, parts of dried Fe/La-Mt were calcined at 500°C for 2 h and the calcined Fe/La-Mt was obtained (C-Fe/La-Mt).

## 2.3. Batch adsorption experiment

Adsorption assays were carried out using batch technique in 250-mL flasks with 100 mL of working volume at pH 6.0, and agitated in a rotary shaker at 160 rpm and 25°C. Samples were taken out at determined time intervals, centrifuged and filtered through 0.22-μm cellulose acetate membrane for the measurement of residual roxarsone. All tests were performed in triplicate.

Adsorption kinetics were investigated by adding 0.1 g of Fe/La-Mt or C-Fe/La-Mt to roxarsone solution (10.0, 20.0, and 40.0 mg L<sup>-1</sup>), and the change of roxarsone concentration with time was measured continuously until the adsorption reached equilibrium state.

The adsorption isotherms at different temperatures (288, 398, and 308 K) were investigated by mixing 0.1 g of Fe/La-Mt or C-Fe/La-Mt with various concentrations of roxarsone solution. The mixtures were agitated for 24 h followed by further analysis.

The effect of pH values on adsorption removal was investigated in the pH range of 2.5–10.0 at initial roxarsone concentration of 20.0 mg L<sup>-1</sup>, and the pH was adjusted using 0.1 mol L<sup>-1</sup> HCl or NaOH. The effect of coexisting anions was investigated by adding 0.1 mmol L<sup>-1</sup> nitrate, sulfate, and phosphate to 26.3 mg L<sup>-1</sup> (0.1 mmol L<sup>-1</sup>) roxarsone solution, respectively. The ionic strength of potassium chloride concentration from 0.1 to 1.0 mol L<sup>-1</sup> at initial roxarsone concentration of 20.0 mg L<sup>-1</sup> was studied. The dosage of the adsorbent for pH, coexisting anions, and ionic strength assays was 0.1 g of Fe/La-Mt.

## 2.4. Analysis

The concentration of roxarsone in the solution was determined using high performance liquid chromatography (HPLC, 1260 Infinity, Agilent Technologies, USA) with a diode array detector at 264 nm, equipping with a Wondasil C18 column (4.6 mm × 150 mm, 5 μm, GL Sciences Inc., Japan) at 30°C for separation. The mobile phase was composed of 50 mmol L<sup>-1</sup> KH<sub>2</sub>PO<sub>4</sub>, methanol, and 0.1% (V/V) formic acid (90:10:0.1, V/V/V) at a flow rate of 1.0 mL min<sup>-1</sup> [13].

The raw and modified clays were characterized using X-ray diffractometer (XRD, D/MAX2500V, Rigaku, Japan), Fourier transform infrared spectrum (FTIR, Nicolette 10, Thermo Fisher, USA), N<sub>2</sub> Brunauer–Emmett–Teller (BET, Tristar II 3020, USA), and field emission scanning electron microscope (FESEM, JEM-2100F, Japan). The XRD analysis was conducted under the condition of Cu Kα radiation (40 kV, 40 mA), and the data were collected in the 2θ range 2°–30° at room temperature. The FTIR spectra were recorded using a mixture of dried clays and fine dried KBr powder in the spectrum range of 4,000–400 cm<sup>-1</sup>. N<sub>2</sub> adsorption isotherms were measured at -196°C, and specific surface area (S<sub>BET</sub>), pore volume, and size distributions were calculated from N<sub>2</sub> adsorption isotherms using Barrett–Joyner–Halenda (BJH) method. The roxarsone-loaded-modified clays were analyzed using X-ray photoelectron spectroscopy (XPS, Escalab 250Xi, Thermo Fisher Scientific, USA).

The adsorbed amount of roxarsone onto modified montmorillonites was calculated based on Eq. (1):

$$q_t = \frac{(C_o - C_t)V}{M} \quad (1)$$

where  $q_t$  is the amount of roxarsone adsorbed by modified montmorillonites at time  $t$ ,  $C_o$  and  $C_t$  are the roxarsone concentrations at initial and time  $t$  in aqueous solution ( $\text{mg L}^{-1}$ ), respectively,  $V$  is the solution volume (L), and  $M$  is the mass of modified montmorillonite used in the experiment (g).

### 3. Results and discussion

#### 3.1. Characterization of natural and modified montmorillonites

Fig. 2(A) shows the XRD patterns of the Ca-Mt (a), Na-Mt (b), Fe/La-Mt (c), and C-Fe/La-Mt (d). The increase in the intensity of peaks indicated that Na-Mt is more crystalline than the raw Ca-Mt. The  $d_{001}$

spacing of Na-Mt appeared at  $5.779^\circ$  ( $d_{001} = 1.53 \text{ nm}$ ), which is in the range of natural montmorillonite [31]. As compared with Ca-Mt and Na-Mt, Fe/La-Mt was less crystalline because there were no well-defined peaks, which can be attributed to the formation of oxocations, and similar result has been reported by Nguyen-Thanh et al. [32]. The un conspicuous 0 0 1 peak in spectra of Fe/La-Mt suggested that the clays were peeled off by interaction with iron species and formed delaminated clays. No diffraction peaks were found in the spectra of C-Fe/La-Mt for the whole phase, implying the loss of crystal in the calcined-modified clays. It could be deduced that the layer structure had undergone dehydroxylation and collapsed after being calcined.

The FTIR spectra of Ca-Mt (e), Fe/La-Mt (f), and C-Fe/La-Mt (g) are shown in Fig. 2(B). As compared with C-Fe/La-Mt, there appeared a peak at  $1,385 \text{ cm}^{-1}$  in the spectra of Fe/La-Mt, which is assigned to the band of  $\text{NO}_3^-$  stretch vibration. An increased peak at  $3,618 \text{ cm}^{-1}$  in the spectra of Ca-Mt is associated with internal hydroxyls of clay minerals, which is a shoulder on a broad asymmetric band centered at  $3,446 \text{ cm}^{-1}$  and is typical for smectites. When the raw materials were modified, the sharp peak disappeared and the broad peak shifted to  $3,442 \text{ cm}^{-1}$ , which could be due to the disruption of hydrogen bond network by diffusing cations. Similar result in the spectra of clays reacting with metal nitrate has been reported before [33]. A strong band at  $1,637 \text{ cm}^{-1}$  found in both raw clays and modified clays, is associated with  $\text{H}_2\text{O}$  plane deformation vibration.

The  $\text{N}_2$  adsorption and desorption isotherms of the original and modified montmorillonites are presented in Fig. 3(A), exhibiting type II shape according to the BDDT classification [34]. The pore size distribution is shown in Fig. 3(B) with average size 3–8 nm. The  $S_{\text{BET}}$  and pore volume increased significantly after the Fe/La-pillared modification, while the average pore size decreased significantly with the modification, as listed in Table 2.

Fig. 4 shows the FESEM images of Ca-Mt (A), Fe/La-Mt (B), and C-Fe/La-Mt (C). It was found that both raw clays and Fe/La-Mt showed highly porous morphology. Obvious difference in microstructure can be seen between the raw clays and Fe/La-Mt. The raw clays presented obvious lamellar structure, while the Fe/La-Mt appeared as slight agglomerates structure, which further confirmed that modified montmorillonite was peeled off after being intercalated. The morphology of C-Fe/La-Mt presented a massive structure, which confirmed the collapse of the structure (Fig. 4(C)).

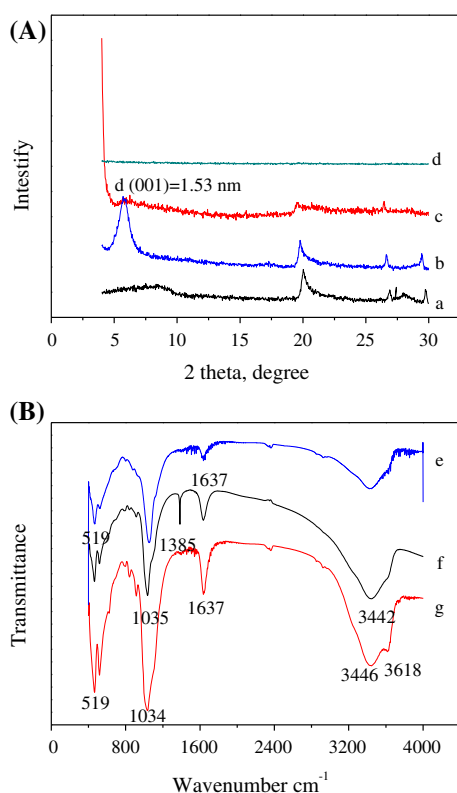


Fig. 2. Spectra of XRD patterns (A): Ca-Mt (a), Na-Mt (b), Fe/La-Mt (c), C-Fe/La-Mt (d), and FTIR patterns (B): Ca-Mt (e), Fe/La-Mt (f), C-Fe/La-Mt (g).

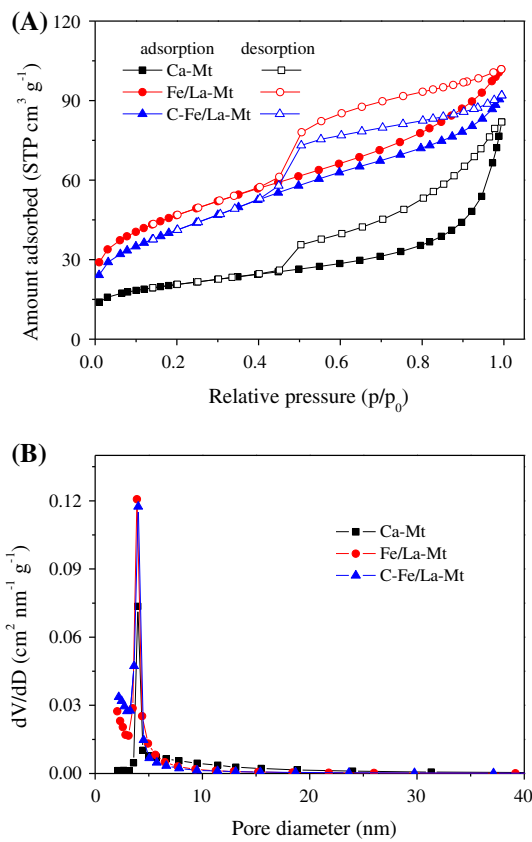


Fig. 3. Nitrogen adsorption–desorption isotherms (A) and mesopore size distribution (B) of Ca-Mt, Fe/La-Mt, and C-Fe/La-Mt.

### 3.2. Effect of contact time

As shown in Fig. 5, the original Ca-Mt exhibited very low adsorption capacity onto roxarsone (Fig. 5(A)), while the modification significantly increased the adsorption capacity (Fig. 5(B)). The adsorption of roxarsone onto Fe/La-Mt (Fig. 5(B)) and C-Fe/La-Mt (Fig. 5(C)) can be divided into two stages, a relatively fast adsorption stage in the first four hours and a slow adsorption stage after that. The fast adsorption of roxarsone was attributed to availability of a large amount of active sites at the external

surfaces of the adsorbent. The adsorption was gradually slowed down when finite adsorption sites were almost occupied by the adsorbate. The adsorption processes approached equilibrium after 20 h of the adsorption for Fe/La-Mt and 24 h for C-Fe/La-Mt at various concentrations investigated. The adsorption capacity at equilibrium state was dependent on the initial concentration. The maximum adsorption capacity increased from 9.77 to 31.87 mg g<sup>-1</sup> for Fe/La-Mt and from 6.51 to 17.19 mg g<sup>-1</sup> for C-Fe/La-Mt, whereas the corresponding removal efficiency decreased from 97.7 to 79.7% for Fe/La-Mt and from 65.1 to 43.0% for C-Fe/La-Mt with the increase in initial roxarsone concentration from 10.0 to 40.0 mg L<sup>-1</sup>. This is because the ratio of available active sites to roxarsone declined with increasing initial roxarsone concentration at the same adsorbent dose, therefore the removal efficiency decreased with increasing initial concentrations of adsorbates. It can be found that the adsorption capacity decreased when the modified clays were calcined, which might be attributed to the collapse of the clay structure. Therefore, Fe/La-Mt is better than C-Fe/La-Mt for the removal of roxarsone from aqueous solution.

### 3.3. Kinetics study

The kinetics and equilibrium isotherm of the adsorption are two important physical and chemical aspects of the process, which are commonly applied to explain the adsorption process. The adsorption kinetics were analyzed using pseudo-first-order and pseudo-second-order models in this study.

The pseudo-first-order model is generally expressed as Eq. (2), and the linear form can be expressed as Eq. (3).

$$\frac{dq_t}{dt} = K_1(q_e - q_t) \quad (2)$$

$$\log(q_e - q_t) = \log q_e - \frac{K_1}{2.303} t \quad (3)$$

Table 2

Structural parameters of original and modified montmorillonites calculated from N<sub>2</sub> adsorption isotherms

Sample	$S_{\text{BET}}$ (m <sup>2</sup> g <sup>-1</sup> )	Pore volume (cm <sup>3</sup> g <sup>-1</sup> )	Average pore diameter (nm)
Ca-Mt	72.42	0.131	7.23
Fe/La-Mt	167.40	0.152	4.09
C-Fe/La-Mt	148.74	0.156	4.00

Note:  $S_{\text{BET}}$ , specific surface area.

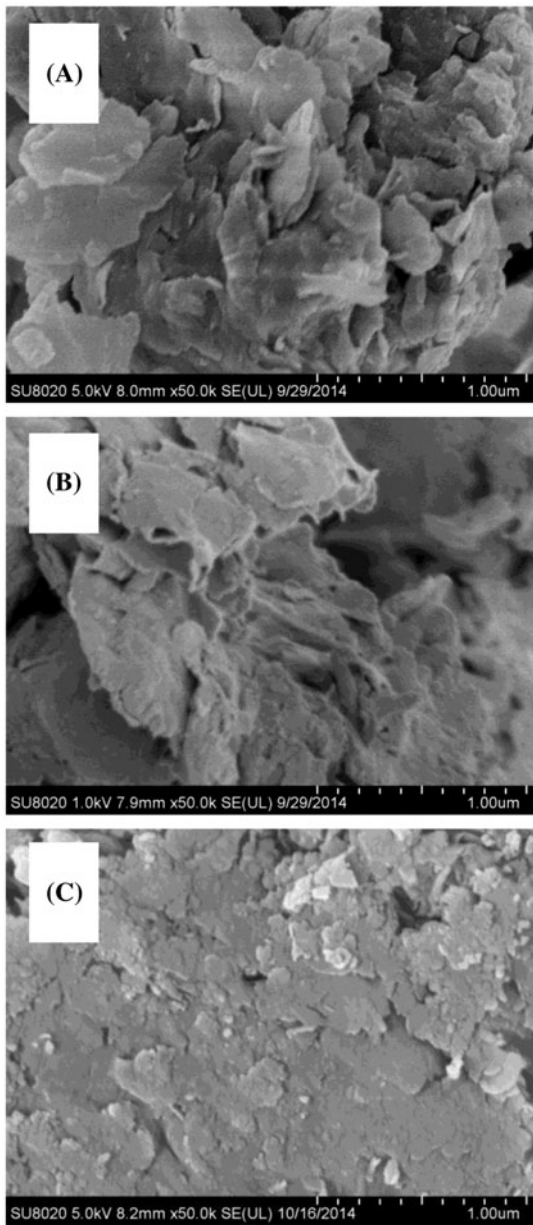


Fig. 4. FESEM images of Ca-Mt (A), Fe/La-Mt (B), and C-Fe/La-Mt (C).

where  $q_e$  and  $q_t$  are the amount of roxarsone adsorbed per unit mass ( $\text{mg g}^{-1}$ ) at equilibrium and time  $t$ , respectively, and  $K_1$  is the rate constant ( $\text{min}^{-1}$ ). The  $q_e$  and  $K_1$  were calculated from the intercepts and the slopes of the plots of  $\log(q_e - q_t)$  vs.  $t$ .

The adsorption process of initial four hours for Fe/La-Mt and C-Fe/La-Mt at various initial roxarsone concentrations were fitted using the pseudo-first-order model, as shown in Fig. 6(A) and (C). The fitting parameters and correlation linear coefficients ( $R^2$ ) obtained are listed in Table 3. The  $R^2$  values of the

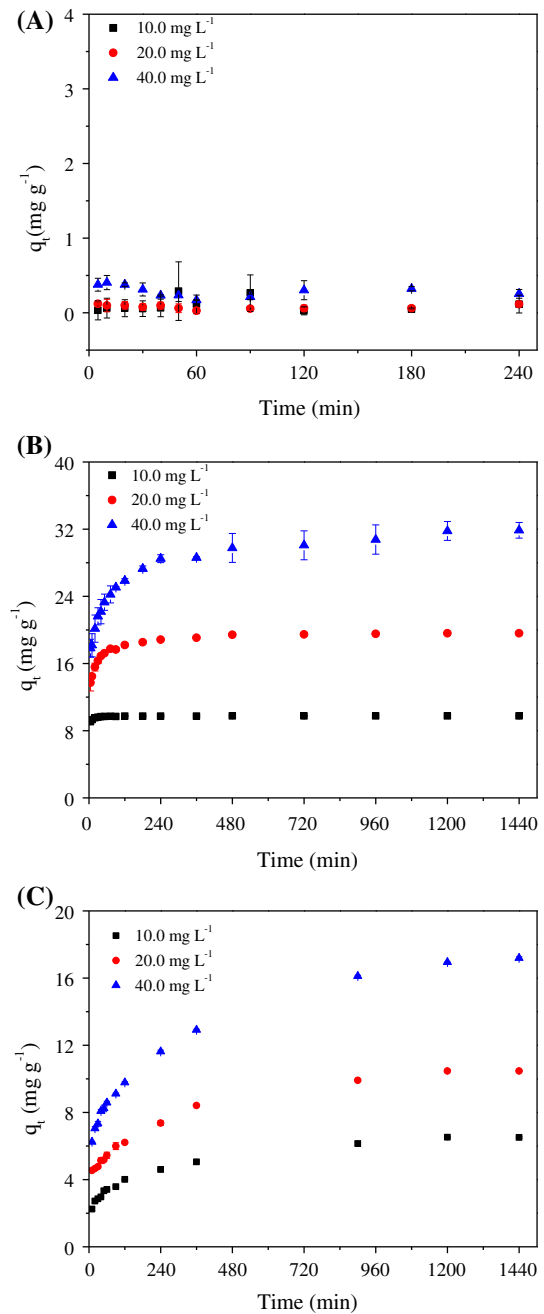


Fig. 5. Adsorption of roxarsone by original Ca-Mt (A), Fe/La-Mt (B), and C-Fe/La-Mt (C) as a function of contact time.

pseudo-first-order model at the investigated concentrations were relatively low for both Fe/La-Mt and C-Fe/La-Mt. In addition, deviations between experimental values and calculated  $q_e$  values began to increase at all concentrations with the prolonging of the adsorption process, showing that pseudo-first-order model cannot well describe the adsorption of

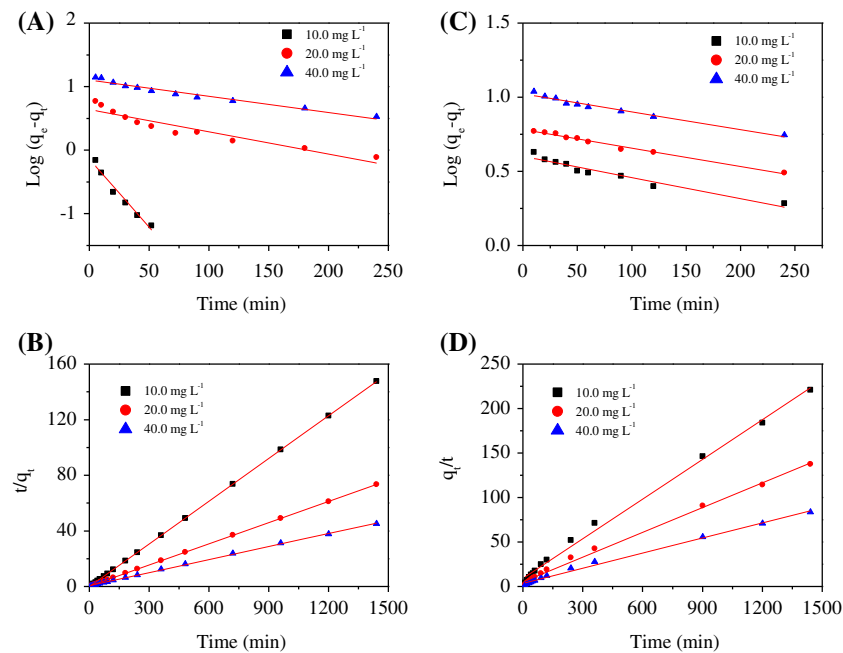


Fig. 6. Adsorption kinetics of roxarsone onto Fe/La-Mt (A and B) and C-Fe/La-Mt (C and D) and fitted with pseudo-first-order model (A and C) and pseudo-second-order model (B and D).

Table 3

Parameters and correlation coefficients of pseudo-first-order and pseudo-second-order of roxarsone adsorption onto Fe/La-Mt and C-Fe/La-Mt

Adsorbent	Initial concentration (mg L <sup>-1</sup> )	Pseudo-first-order			Pseudo-second-order		
		$K_1 \times 10^{-3}$ (min <sup>-1</sup> )	$q_e$ (mg g <sup>-1</sup> )	$R^2$	$K_2 \times 10^{-3}$ (g mg <sup>-1</sup> min <sup>-1</sup> )	$q_e$ (mg g <sup>-1</sup> )	$R^2$
Fe/La-Mt	10.0	49.55	0.73	0.960	243.40	9.76	1.000
	20.0	8.09	4.39	0.890	6.69	19.72	1.000
	40.0	5.88	12.74	0.963	1.41	31.94	0.999
C-Fe/La-Mt	10.0	5.87	4.00	0.936	2.40	6.72	0.996
	20.0	6.83	6.04	0.987	1.56	10.79	0.996
	40.0	8.51	10.54	0.967	0.84	17.68	0.994

roxarsone onto the modified clays. Therefore, pseudo-second-order model was tried to describe the adsorption process.

Pseudo-second-order kinetics model was presented in Eq. (4), and its linear form was expressed in Eq. (5).

$$\frac{dq_t}{dt} = K_2(q_e - q_t)^2 \quad (4)$$

$$\frac{t}{q_t} = \frac{1}{K_2 q_e^2} - \frac{1}{q_e} t \quad (5)$$

where  $q_t$  and  $q_e$  have the same mean as mentioned in Eq. (2), and  $K_2$  is the rate constant of pseudo-second-order kinetic model (g mg<sup>-1</sup> min<sup>-1</sup>). The  $q_e$  and  $K_2$  were calculated from the slope and the intercept of the plots of  $t/q_t$  vs.  $t$ .

Fig. 6(B) and (D) shows the plots of the pseudo-second-order model, and the fitting parameters and correlation coefficients are also presented in Table 3. The pseudo-second-order model showed that the simulated  $q_e$  values had good agreement with the experimental  $q_e$  values for both Fe/La-Mt and C-Fe/La-Mt, indicating that pseudo-second-order model is better than pseudo-first-order model for explaining the adsorption process.

### 3.4. Adsorption isotherm analysis

To explore the interaction between roxarsone and modified montmorillonites, two most commonly used adsorption isotherms, the Langmuir and Freundlich isotherms are selected to elucidate the adsorption process at the solid–liquid surface. The Langmuir adsorption isotherm is based on the theory of monomolecular adsorption with the assumption that each active site can only adsorb one solvent or solute molecule. The linear equation of the Langmuir isotherm is expressed as Eq. (6):

$$\frac{C_e}{q_e} = \frac{1}{q_m K_L} + \frac{C_e}{q_m} \quad (6)$$

where  $C_e$  is the equilibrium concentration of roxarsone in solution ( $\text{mg L}^{-1}$ ),  $q_e$  has the same meaning as described above,  $q_m$  ( $\text{mg g}^{-1}$ ) and  $K_L$  ( $\text{L mg}^{-1}$ ) are the Langmuir isotherm constants representing the maximum theoretical adsorption capacity and the affinity of adsorption sites, respectively.

The essential parameter  $R_L$  of the Langmuir isotherm is a dimensionless equilibrium parameter and can be obtained:

$$R_L = \frac{1}{1 + K_L C_0} \quad (7)$$

where the value of  $K_L$  can be obtained from the Langmuir isotherm, and the value of  $R_L$  was calculated at the initial roxarsone concentration of  $5.0 \text{ mg L}^{-1}$ .

While the Freundlich isotherm is based on multi-layer adsorption with the heterogeneous surfaces of the adsorbent. The linear form of Freundlich isotherm is expressed as Eq. (8):

$$\log q_e = \log K_F + \frac{1}{n} \log C_e \quad (8)$$

where  $K_F$  relates to the adsorption capacity ( $\text{mg g}^{-1}$ ) and  $n$  ( $\text{L g}^{-1}$ ) is an empirical parameter relating to adsorption intensity.

Fig. 7(A)–(C) shows the experimental data at equilibrium time as well as linear plots of the Langmuir and Freundlich isotherms for Fe/La-Mt, while Fig. 7(D)–(F) for C-Fe/La-Mt. The fitting parameters and correlation coefficients ( $R^2$ ) at three different temperatures are listed in Table 4. The results showed that the Langmuir isotherm was more appropriate than the Freundlich isotherm for Fe/La-Mt and C-Fe/La-Mt with  $R^2$  values all above 0.990, indicating that the sorption of roxarsone onto Fe/La-Mt and C-Fe/

La-Mt can be well interpreted using Langmuir isotherm. The  $q_m$  varied from 31.07 to 36.83 for Fe/La-Mt, indicating that the adsorption capacity of Fe/La-Mt is higher than  $\text{TiO}_2$  [12] and modified carbon nanotubes [29] but lower than iron and aluminum oxides [36] for roxarsone adsorption. The calculated values of  $K_L$  were less than 1, which implied the adsorption of roxarsone onto Fe/La-Mt and C-Fe/La-Mt was a favorable process [35]. All of the values of adsorption intensity  $n$  at three different temperatures were  $>1$ , suggesting that the adsorption was mainly a physical process.

### 3.5. Thermodynamic analysis

Thermodynamic analysis can be used to better understand the degree and drive force of adsorption process, and further analyze various factors affecting the adsorption. Thermodynamic analysis was conducted by investigating the sorption of  $40.0 \text{ mg L}^{-1}$  roxarsone onto  $0.1 \text{ g}$  of Fe/La-Mt at the temperatures of 15, 25, and  $35^\circ\text{C}$ , respectively. The thermodynamic parameters such as Gibbs energy ( $\Delta G^\circ$ ), enthalpy changes ( $\Delta H^\circ$ ), and entropy changes ( $\Delta S^\circ$ ) were calculated using Eqs. (9) and (10), respectively.

$$\Delta G^\circ = -RT \ln K_c \quad (9)$$

$$\ln K_c = \frac{\Delta S^\circ}{R} - \frac{\Delta H^\circ}{RT} \quad (10)$$

where  $K_c$  represents the equilibrium constant and  $R$  is the universal gas constant ( $8.314 \text{ J mol}^{-1} \text{ K}^{-1}$ ). The thermodynamic parameters are listed in Table 5. The values of  $\Delta G^\circ$  calculated at different temperatures were in the range of  $-5.008$  to  $-0.802 \text{ kJ mol}^{-1}$ , suggesting that the interaction between roxarsone and modified montmorillonites was spontaneous and involved in physical adsorption [35]. Additionally, the less negative values of  $\Delta G^\circ$  at the lower temperatures suggested a smaller drive force of the adsorption process. The drive force is relatively lower for C-Fe/La-Mt than that for Fe/La-Mt at the same temperature. The positive values of  $\Delta H^\circ$  implied the strong interaction between roxarsone and the modified clay during the adsorption process. The positive values of  $\Delta S^\circ$  indicated the increased randomness at the solid–solution interface with increasing temperature [35].

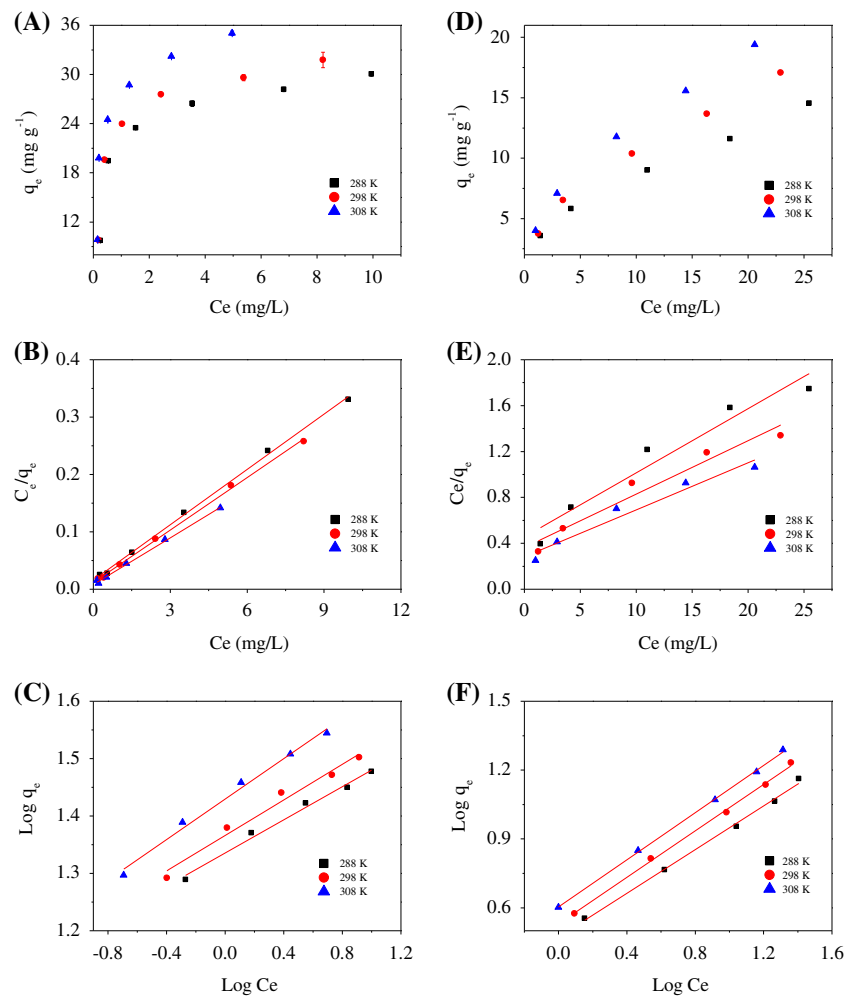


Fig. 7. Adsorption isotherms of roxarsone onto Fe/La-Mt (A) and C-Fe/LA-Mt (D) at different temperatures and fitted with the Langmuir model (B and E) and the Freundlich model (C and F).

Table 4

Isotherm parameters for the adsorption of roxarsone onto Fe/La-Mt and Fe/La-Mt at different temperatures

Adsorbent	Temperature (K)	Langmuir isotherm				Freundlich isotherm		
		$q_m$ (mg g <sup>-1</sup> )	$K_L$ (L mg <sup>-1</sup> )	$R_L$	$R^2$	$n$	$K_F$ (mg g <sup>-1</sup> )	$R^2$
Fe/La-Mt	288	31.07	2.00	0.090	0.998	6.91	21.67	0.986
	298	32.82	2.53	0.073	0.998	6.46	23.25	0.972
	308	36.83	3.22	0.058	0.997	5.67	26.91	0.987
C-Fe/La-Mt	288	17.88	0.12	0.621	0.998	2.10	2.97	0.995
	298	21.47	0.13	0.610	0.998	1.97	3.40	0.997
	308	24.39	0.14	0.580	0.997	1.95	4.02	0.999

### 3.6. Effect of environmental conditions

Fig. 7(A) shows the influence of pH on the roxarsone adsorption by Fe/La-Mt at the initial concentration of 20 mg L<sup>-1</sup>. The pH in solution can affect the

degree of ionization, speciation of ionizable chemicals, and surface charge of adsorbents [36]. The adsorption efficiency of ionizable chemicals at the solid-liquid interfaces is highly dependent on the pH of aqueous

Table 5  
Thermodynamic parameters for roxarsone adsorption onto Fe/La-Mt and C-Fe/La-Mt

Adsorbent	Temperature (K)	$\Delta G^\circ$ (kJ mol <sup>-1</sup> )	$\Delta H^\circ$ (kJ mol <sup>-1</sup> )	$\Delta S^\circ$ (kJ K <sup>-1</sup> mol <sup>-1</sup> )	$R^2$
Fe/La-Mt	288	-2.649	31.17	116.91	0.943
	298	-3.356			
	308	-5.008			
C-Fe/La-Mt	288	-0.802	20.32	73.38	0.999
	298	-1.520			
	308	-2.121			

solution [36]. As shown in Fig. 8(A), the adsorption capacity was relatively high at low pH values, and the maximum adsorption occurred at pH 2.5 in the investigated pH range. The adsorption capacity reduced slightly when pH values increased from 2.5 to 8.0, thereafter declined sharply as pH increased from 8.0 to 10.0. At pH 2.5, the adsorption capacity was 19.70 mg g<sup>-1</sup>, which reduced to 13.36 mg g<sup>-1</sup> at pH 10.0.

The effect of pH values on the adsorption of roxarsone onto Fe/La-Mt may be attributed to the pK<sub>a</sub> values of adsorbates and the point of zero charges (pH<sub>pzc</sub>) of the adsorbent. Roxarsone is a kind of organic arsenic compound with the pK<sub>a</sub> values of 3.49, 5.74, and 9.13, respectively [37]. The increase in pH values in aqueous solution led to increasing ionization. When the pH value of aqueous solution is above 9.13, roxarsone is negatively charged. The pH<sub>pzc</sub> value of modified montmorillonite was around 5.2, which is negatively charged at pH > pH<sub>pzc</sub> [38]. Due to the negatively charged roxarsone and the negatively charged surface of the modified clays at high pH values, the removal efficiency declined with the increase in pH in aqueous solution.

Roxarsone is a negatively charged compound under normal conditions, other negatively charged anions, such as nitrate, phosphate, and sulfate in natural water may compete with roxarsone for active sites of adsorbents. Fig. 8(B) shows the effect of three kinds of anions on the adsorption removal of roxarsone through Fe/La-Mt. It can be found that the presence of NO<sub>3</sub><sup>-</sup> and SO<sub>4</sub><sup>2-</sup> had no noticeable influence on the adsorption of roxarsone, while PO<sub>4</sub><sup>3-</sup> greatly decreased the removal of roxarsone. The adsorption capacity of roxarsone reduced from 24.97 to 17.96 mg g<sup>-1</sup> in the presence of PO<sub>4</sub><sup>3-</sup>. Many studies have reported that phosphate reduced the adsorption of arsenate compounds onto minerals [39–41]. The inhibition to the adsorption of roxarsone onto clays was attributed to the competition for the limited active sites between roxarsone and phosphate, because arsenic and

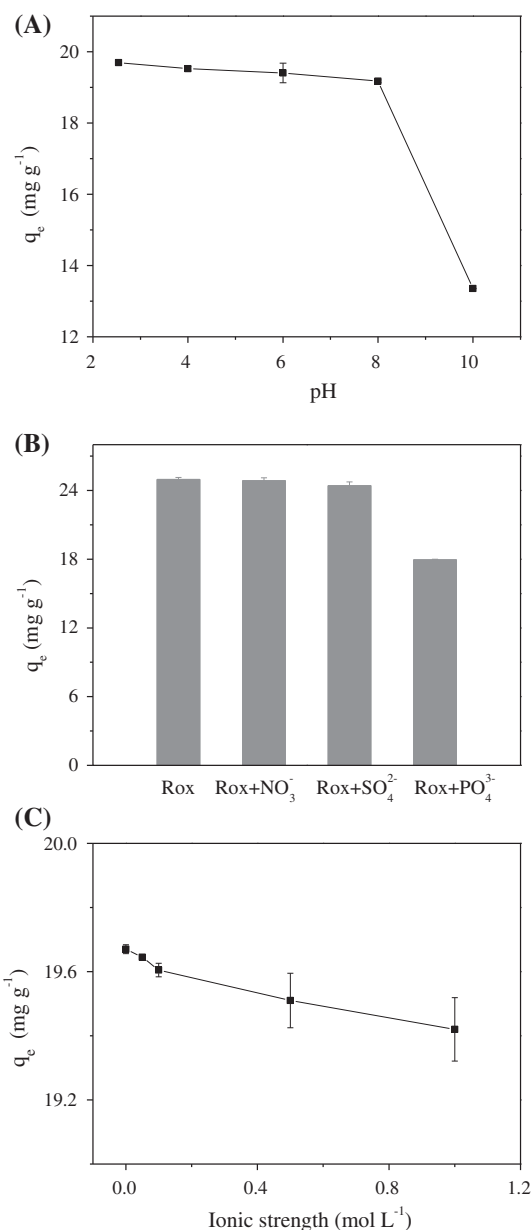


Fig. 8. Effect of pH (A), coexisting anions (B), and ionic strength (C) on the roxarsone adsorption by Fe/La-Mt.

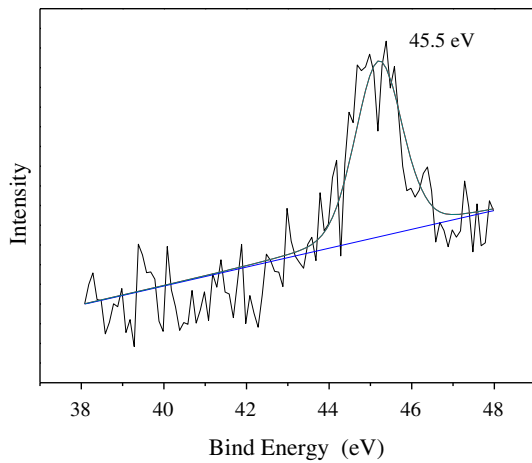


Fig. 9. As 3d XPS spectra of roxarsone-loaded Fe/La-Mt.

phosphate have similar structure and chemical reactivities [6].

Fig. 8(C) shows the effect of ionic strength on roxarsone adsorption by Fe/La-Mt. It can be found that the adsorption efficiency of Fe/La-Mt slightly decreased with the increase in KCl concentrations. It

has been reported that if the adsorption capacity is affected by ionic strength, the outer-sphere complexation may be a predominant role for the adsorption [42,43]. The present result suggested that the adsorption of roxarsone onto Fe/La-Mt mainly involved outer-sphere complexation, while previous researches have shown that arsenic species formed inner-sphere complexes with various minerals [6,25,44].

### 3.7. XPS analysis

The roxarsone-loaded Fe/La-Mt was characterized using XPS, as shown in Figs. 9 and 10. The characteristic peak appeared at binding energy of 45.5 eV can be assigned to the atom of arsenate [45]. The fact that arsenic in roxarsone in the form of pentavalence suggests the valence of arsenic was kept unchanged during the adsorption process. In addition, high-resolution spectra of C 1s and O 1s region were also analyzed and deconvoluted according to Lim et al. [45]. The results are listed in Table 6. The relative content of metal oxide content increased from 1.5 to 2.1% and C–C bond increased from 56.3 to 68.4%. The results confirmed that roxarsone was absorbed onto the surface of Fe/La-Mt.

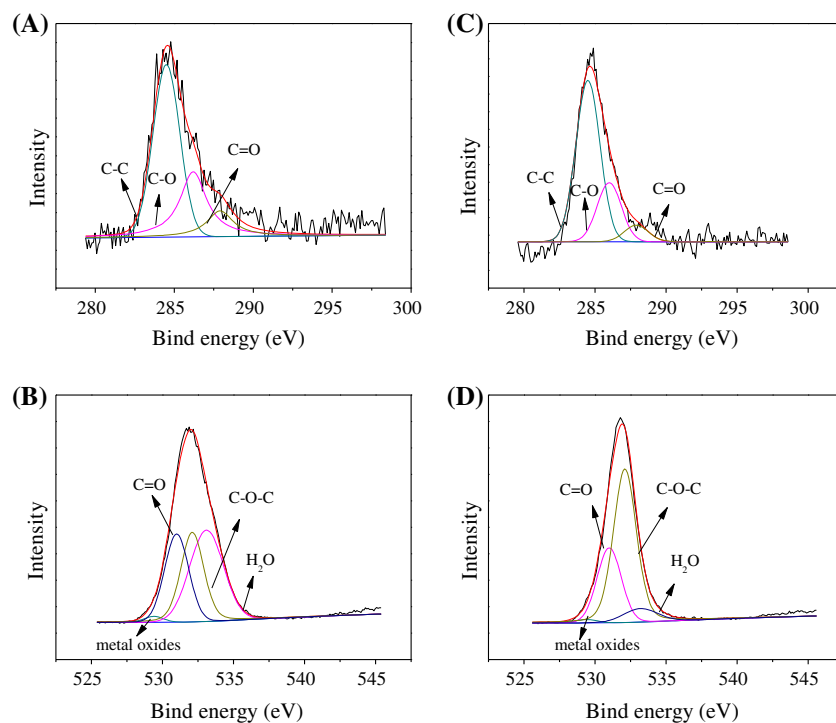


Fig. 10. C 1s XPS spectra of original Fe/La-Mt (A) and roxarsone-loaded Fe/La-Mt (B); O 1s XPS spectra of original Fe/La-Mt (C) and roxarsone-loaded Fe/La-Mt (D).

Table 6  
Binding energy and relative content of As, O, and C in roxarsone-loaded Fe/La-Mt

Valence state	Sample	Proposed component	Binding energy (eV)	Relative content (%)
As 3d	Roxarsone-loaded Fe/La-Mt	As (V)	52.5	100
O 1s	Fe/La-Mt	Metal oxide	529.4	1.5
		C=O	531	28.2
		C–OH, C–O–C	532.1	29.7
		H–O–H	533.1	40.6
	Roxarsone-loaded Fe/La-Mt	Metal oxide	529.4	2.6
		C=O	531	70.8
		C–OH, C–O–C	532.1	8.8
		H–O–H	533.1	17.7
C–(C, H)	Fe/La-Mt	C–C	284.5	56.3
		C–OH, C–O–C	286	31.4
		C=O	287.9	12.4
		C–C	284.5	68.4
	Fe/La-Mt-As	C–OH, C–O–C	286	24.7
		C=O	287.9	6.9

#### 4. Conclusions

Fe/La-pillared montmorillonite was prepared as an absorbent for the removal of roxarsone from aqueous solution. BET analysis confirmed the increase in specific surface area and pore volume after the Fe/La-pillared modification. FESEM analysis of Fe/La-Mt and C-Fe/La-Mt showed that the clays were peeled off after being modified, while collapsed structure was formed after being calcined. The kinetics of roxarsone adsorption onto both Fe/La-Mt and C-Fe/La-Mt can be better described using the pseudo-second-order model. The adsorption isotherms analysis showed that roxarsone adsorption onto modified montmorillonites can be well interpreted using the Langmuir model. The result of thermodynamic analysis suggested the adsorption was a spontaneous and endothermic process. The adsorption capacity reduced slightly when solution pH values increased from 2.5 to 8.0 but decreased sharply as pH further increased from 8.0 to 10.0. The adsorption removal of roxarsone by Fe/La-Mt in aqueous solution decreased markedly in the existence of phosphate ions and was dependent slightly on ionic strength. The XPS results confirmed that roxarsone was loaded onto the surface of Fe/La-Mt. The high adsorption capacity of roxarsone in a wide pH range demonstrated that Fe/La-Mt can be used economically for the removal of roxarsone from aqueous solution.

#### Acknowledgements

This research was partly supported by the NSFC (51578205, 51538012), the Science and Technology

Innovation Fund from Beijing Academy of Agriculture and Forestry Sciences (CXJJ201317), and the Program for Cultivating Excellent Talents in Beijing (2013D002020000001).

#### References

- [1] K.E. Nachman, P.A. Baron, G. Raber, K.A. Francesconi, A. Navas-Acien, D.C. Love, Roxarsone, inorganic arsenic, and other arsenic species in chicken: A U.S.-based market basket sample, *Environ. Health Perspect.* 121 (2013) 818–824.
- [2] F.F. Zhang, W. Wang, S.J. Yuan, Z.H. Hu, Biodegradation and speciation of roxarsone in an anaerobic granular sludge system and its impacts, *J. Hazard. Mater.* 279 (2014) 562–568.
- [3] B.P. Jackson, J.C. Seaman, P.M. Bertsch, Fate of arsenic compounds in poultry litter upon land application, *Chemosphere* 65 (2006) 2028–2034.
- [4] J.R. Garbarino, A.J. Bednar, D.W. Rutherford, R.S. Beyer, R.L. Wershaw, Environmental fate of roxarsone in poultry litter. I. Degradation of roxarsone during composting, *Environ. Sci. Technol.* 37 (2003) 1509–1514.
- [5] A.J. Bednar, J.R. Garbarino, I. Ferrer, D.W. Rutherford, R.L. Wershaw, J.F. Ranville, T.R. Wildeman, Photodegradation of roxarsone in poultry litter leachates, *Sci. Total Environ.* 302 (2003) 237–245.
- [6] W.R. Chen, C.H. Huang, Surface adsorption of organoarsenic roxarsone and arsanilic acid on iron and aluminum oxides, *J. Hazard. Mater.* 227–228 (2012) 378–385.
- [7] Z.M. Sun, Y.C. Yu, S.Y. Pang, D.Y. Du, Manganese-modified activated carbon fiber (Mn-ACF): Novel efficient adsorbent for Arsenic, *Appl. Surf. Sci.* 284 (2013) 100–106.
- [8] WHO. Guidelines for Drinking-Water Quality: First Addendum to Volume 1, Recommendations, World Health Organization, 2006.

- [9] T. Basu, U.C. Ghosh, Nano-structured iron(III)-cerium (IV) mixed oxide: Synthesis, characterization and arsenic sorption kinetics in the presence of co-existing ions aiming to apply for high arsenic groundwater treatment, *Appl. Surf. Sci.* 283 (2013) 471–481.
- [10] T. Budinova, D. Savova, B. Tsyntsarski, C.O. Ania, B. Cabal, J.B. Parra, N. Petrov, Biomass waste-derived activated carbon for the removal of arsenic and manganese ions from aqueous solutions, *Appl. Surf. Sci.* 255 (2009) 4650–4657.
- [11] B.K. Jung, J.W. Jun, Z. Hasan, S.H. Jhung, Adsorptive removal of p-arsanilic acid from water using mesoporous zeolitic imidazolate framework-8, *Chem. Eng. J.* 267 (2015) 9–15.
- [12] S. Zheng, W.J. Jiang, Y. Cai, D.D. Dionysiou, K.E. O'Shea, Adsorption and photocatalytic degradation of aromatic organoarsenic compounds in TiO<sub>2</sub> suspension, *Catal. Today* 224 (2014) 83–88.
- [13] D.L. Lu, F. Ji, W. Wang, S.J. Yuan, Z.H. Hu, T.H. Chen, Adsorption and photocatalytic decomposition of roxarsone by TiO<sub>2</sub> and its mechanism, *Environ. Sci. Pollut. Res.* 21 (2014) 8025–8035.
- [14] H.L. Wang, Z.H. Hu, Z.L. Tong, Q. Xu, W. Wang, S.J. Yuan, Effect of arsenic acid on anaerobic methanogenic process: Kinetics, inhibition and biotransformation analysis, *Biochem. Eng. J.* 91 (2014) 179–185.
- [15] L. Shi, W. Wang, S.J. Yuan, Z.H. Hu, Electrochemical stimulation of microbial roxarsone degradation under anaerobic conditions, *Environ. Sci. Technol.* 48 (2014) 7951–7958.
- [16] H. Liu, G.Q. Wang, J. Ge, L. Liu, G.W. Chen, Fate of roxarsone during biological nitrogen removal process in wastewater treatment systems, *Chem. Eng. J.* 255 (2014) 500–505.
- [17] C.O. Cope, D.S. Webster, D.A. Sabatini, Arsenate adsorption onto iron oxide amended rice husk char, *Sci. Total Environ.* 488 (2014) 558–565.
- [18] I.A. Lawal, B. Moodley, Synthesis, characterisation and application of imidazolium based ionic liquid modified montmorillonite sorbents for the removal of amaranth dye, *RSC Adv.* 5 (2015) 61913–61924.
- [19] H.W. Fan, L.M. Zhou, X.H. Jiang, Q. Huang, W.C. Lang, Adsorption of Cu<sup>2+</sup> and methylene blue on dodecyl sulfobetaine surfactant-modified montmorillonite, *Appl. Clay Sci.* 95 (2014) 150–158.
- [20] M. Kiranşan, R.D.C. Soltani, A. Hassani, S. Karaca, A. Khataee, Preparation of cetyltrimethylammonium bromide modified montmorillonite nanomaterial for adsorption of a textile dye, *J. Taiwan Inst. Chem. Eng.* 45 (2014) 2565–2577.
- [21] H. Long, P.X. Wu, N.W. Zhu, Evaluation of Cs<sup>+</sup> removal from aqueous solution by adsorption on ethylamine-modified montmorillonite, *Chem. Eng. J.* 225 (2013) 237–244.
- [22] X.H. Ren, Z.L. Zhang, H.J. Luo, B.J. Hu, Z. Dang, C. Yang, L.Y. Li, Adsorption of arsenic on modified montmorillonite, *Appl. Clay Sci.* 97–98 (2014) 17–23.
- [23] K.Z. Setshedi, M. Bhaumik, M.S. Onyango, A. Maity, Breakthrough studies for Cr(VI) sorption from aqueous solution using exfoliated polypyrrole-organically modified montmorillonite clay nanocomposite, *J. Ind. Eng. Chem.* 20 (2014) 2208–2216.
- [24] P.X. Wu, Q. Zhang, Y.P. Dai, N.W. Zhu, Z. Dang, P. Li, J.H. Wu, X.D. Wang, Adsorption of Cu(II), Cd(II) and Cr(III) ions from aqueous solutions on humic acid modified Ca-montmorillonite, *Geoderma* 164 (2011) 215–219.
- [25] P. Na, X. Jia, B. Yuan, Y. Li, J. Na, Y. Chen, L. Wang, Arsenic adsorption on Ti-pillared montmorillonite, *J. Chem. Technol. Biotechnol.* 85 (2010) 708–714.
- [26] S. Tokunaga, S.A. Wasay, S.-W. Park, Removal of arsenic(V) ion from aqueous solutions by lanthanum compounds, *Water Sci. Technol.* 35 (1997) 71–78.
- [27] V. Kuroki, G.E. Bosco, P.S. Fadini, A.A. Mozeto, A.R. Cestari, W.A. Carvalho, Use of a La(III)-modified bentonite for effective phosphate removal from aqueous media, *J. Hazard. Mater.* 274 (2014) 124–131.
- [28] S.P. Kamble, P. Dixit, S.S. Rayalu, N.K. Labhsetwar, Defluoridation of drinking water using chemically modified bentonite clay, *Desalination* 249 (2009) 687–693.
- [29] J. Hu, Z. Tong, G. Chen, X. Zhan, Z. Hu, Adsorption of roxarsone by iron (hydr)oxide-modified multi-walled carbon nanotubes from aqueous solution and its mechanisms, *Int. J. Environ. Sci. Technol.* 11 (2014) 785–794.
- [30] P. Yuan, H.P. He, F. Bergaya, D.Q. Wu, Q. Zhou, J.X. Zhu, Synthesis and characterization of delaminated iron-pillared clay with meso-microporous structure, *Microporous Mesoporous Mater.* 88 (2006) 8–15.
- [31] M.E. Parolo, M.J. Avena, M.C. Savini, M.T. Baschini, V. Nicotra, Adsorption and circular dichroism of tetracycline on sodium and calcium-montmorillonites, *Colloids Surf., A* 417 (2013) 57–64.
- [32] D. Nguyen-Thanh, K. Block, T.J. Bandosz, Adsorption of hydrogen sulfide on montmorillonites modified with iron, *Chemosphere* 59 (2005) 343–353.
- [33] S. Srinivasan, S. Ganguly, FT-IR spectroscopic studies of metal nitrates supported on a modified montmorillonite clay, *Catal. Lett.* 10 (1991) 279–287.
- [34] S. Brunauer, L.S. Deming, W.E. Deming, E. Teller, On a theory of the van der Waals adsorption of gases, *J. Am. Chem. Soc.* 62 (1940) 1723–1732.
- [35] V. Vimonses, S.M. Lei, B. Jin, C.W.K. Chow, C. Saint, Kinetic study and equilibrium isotherm analysis of Congo Red adsorption by clay materials, *Chem. Eng. J.* 148 (2009) 354–364.
- [36] L. Zeng, X. Li, J. Liu, Adsorptive removal of phosphate from aqueous solutions using iron oxide tailings, *Water Res.* 38 (2004) 1318–1326.
- [37] Z. Qiang, C. Adams, Potentiometric determination of acid dissociation constants (pK<sub>a</sub>) for human and veterinary antibiotics, *Water Res.* 38 (2004) 2874–2890.
- [38] A. Ramesh, H. Hasegawa, T. Maki, K. Ueda, Adsorption of inorganic and organic arsenic from aqueous solutions by polymeric Al/Fe modified montmorillonite, *Sep. Purif. Technol.* 56 (2007) 90–100.
- [39] Y. Gao, A. Mucci, Individual and competitive adsorption of phosphate and arsenate on goethite in artificial seawater, *Chem. Geol.* 199 (2003) 91–109.
- [40] M. Streat, K. Hellgardt, N.L.R. Newton, Hydrated ferrous oxide as an adsorbent in water treatment, *Process Saf. Environ. Prot.* 86 (2008) 21–30.

- [41] Z. Ren, G. Zhang, J. Paul Chen, Adsorptive removal of arsenic from water by an iron–zirconium binary oxide adsorbent. *J. Colloid Interface Sci.* 358 (2011) 230–237.
- [42] J. Su, H.-G. Huang, X.-Y. Jin, X.-Q. Lu, Z.-L. Chen, Synthesis, characterization and kinetic of a surfactant-modified bentonite used to remove As(III) and As(V) from aqueous solution, *J. Hazard. Mater.* 185 (2011) 63–70.
- [43] K. Hayes, J. Leckie, Modeling ionic strength effects on cation adsorption at hydrous oxide/solution interfaces, *J. Colloid Interface Sci.* 115 (1987) 564–572.
- [44] Y. Gao, A. Mucci, Acid base reactions, phosphate and arsenate complexation, and their competitive adsorption at the surface of goethite in 0.7 M NaCl solution, *Geochim. Cosmochim. Acta* 65 (2001) 2361–2378.
- [45] S.F. Lim, Y.M. Zheng, J.P. Chen, Organic arsenic adsorption onto a magnetic sorbent, *Langmuir* 25 (2009) 4973–4978.